Journal of Molecular Catalysis A: Chemical 335 (2011) 189–198

Contents lists available at ScienceDirect

Journal of Molecular Catalysis A: Chemical

journal homepage: www.elsevier.com/locate/molcata

Effect of acid treatment on the surface of multiwalled carbon nanotubes prepared from Fe–Co supported on $CaCO_3$: Correlation with Fischer–Tropsch catalyst activity

Myriam A.M. Motchelaho[a,b], Haifeng Xiong[b,c], Mahluli Moyo[a,b], Linda L. Jewell[a,*], Neil J. Coville[b,c,**]

[a] School of Chemical and Metallurgical Engineering, University of the Witwatersrand, Johannesburg 2050, South Africa
[b] Molecular Sciences Institute, School of Chemistry, University of the Witwatersrand, Johannesburg 2050, South Africa
[c] DST/NRF Centre of Excellence in Strong Materials, University of the Witwatersrand, Johannesburg 2050, South Africa

ARTICLE INFO

Article history:
Received 1 July 2010
Received in revised form 2 November 2010
Accepted 26 November 2010
Available online 9 December 2010

Keywords:
Iron–cobalt catalyst
$CaCO_3$ support
Fischer–Tropsch activity
Multiwalled carbon nanotubes

ABSTRACT

Carbon nanotubes (CNTs) were obtained through the catalytic decomposition of C_2H_2 at 700 °C over Fe–Co supported on $CaCO_3$ and confirmed by TEM to be composed of multiwalled carbon nanotubes. The CNTs were refluxed in 30% and 55% HNO_3 for 2 and 6 h in order to remove impurities and introduce oxygen surface groups. This rendered the CNTs less hydrophobic. The morphology, microstructure, surface area, pore volume and surface chemical properties of the acid treated CNTs were analysed by TEM, N_2 physisorption, TGA, FTIR, Raman spectroscopy and zeta potential measurements. The surface roughness, together with the degree of surface functionalization correlated with the harshness (time and concentration) of the acid treatment. Fischer–Tropsch synthesis studies (275 °C, 8 bar) were performed on all the Fe loaded (10%)/CNT catalysts and activity studies revealed that the more severe the acid treatment the higher the activity of the catalysts.

1. Introduction

Carbon materials with various morphologies are widely used as adsorbents, as catalysts and/or catalyst supports and for structural reinforcement of polymers. The carbons often have relatively high surface areas, high thermal stability and show chemical inertness. Their surface chemistry, especially the presence of oxygen functionalities determines the application of the material [1,2]. Historically activated carbons and carbon blacks are the most commonly used forms of carbon used in industry. More recently the use of carbon nanotubes, fullerenes and related materials in high-tech applications has attracted growing interest [3,4].

Carbon nanotubes, popularised by studies by Iijima [5], represent one of the best examples of nanostructures derived from bottom-up chemical synthesis approaches [6]. Both single walled carbon nanotubes (SWCNTs) and multiwalled carbon nanotubes (MWCNTs) have a simple chemical composition and atomic bonding configuration but exhibit an extreme diversity and richness among nanomaterials in terms of structure and structure–property relations [7].

The synthesis, purification, properties, manipulation and more recently, the chemistry of nanotubes are all subjects of intensive investigations. There are three common methods used to make CNTs: laser ablation [8], electric arc discharge [9,10] and chemical vapour deposition [11–14]. Catalytic chemical vapour deposition (CCVD) has proven to be an excellent method for large-scale production of high quality MWCNTs at relatively low cost [15–17]. By employing specific catalyst and carbon sources it is possible to control the structural characteristics of CNTs when CCVD is used [18].

The CCVD synthesis method consists of decomposing a carbon-containing gas over a supported catalyst. In order to improve the yield and quality of CNT production, various metal catalysts, supports and carbon sources have been investigated [19,20]. The most widely used metals are Fe, Co and Ni as well as the alloys of these nanoparticles [21,22]. Conventional supports such as SiO_2, Al_2O_3, and zeolite have been successfully used in the synthesis of CNTs but purification of the product has proven to be difficult. A detailed study by Magrez et al. [16] showed that $CaCO_3$ is an excellent support for CNT synthesis because of the good match

Abbreviations: CNT, carbon nanotubes; MWCNT, multiwalled carbon nanotubes; SWCNT, sinlge walled carbon nanotubes.

* Corresponding author. Tel.: +27 11 717 7507.
** Corresponding author. Tel.: +27 11 717 6738; fax: +27 11 717 6749.
E-mail addresses: linda.jewell@wits.ac.za (L.L. Jewell), neil.coville@wits.ac.za (N.J. Coville).

1381-1169/$ – see front matter © 2010 Elsevier B.V. All rights reserved.
doi:10.1016/j.molcata.2010.11.033

between the carbonate decomposition temperature and the nanotube growth. Residual CaO support can be easily be removed by a one step acid treatment [23,15]. Earlier studies [19,23] revealed that the order of catalyst activity in the CVD synthesis was Fe–Co/$CaCO_3$ ≫ Co/$CaCO_3$ > Fe/$CaCO_3$. The Fe–Co bimetallic system supported on $CaCO_3$ was therefore used in this present study.

Regardless of the method used to make CNTs, there is always a significant amount of impurity present in the final product (graphitic debris, catalyst particles and fullerenes) [24]. These impurities often influence the desired properties of the CNTs. It is therefore important to both evaluate and reduce or completely eliminate impurities in the as-grown CNTs. Although there are many suggested methods for CNT purification, oxidation with concentrated HNO_3 or HNO_3–H_2SO_4 is the most widely used [1,25–29]. However no purification method that fulfils all the requirements for technical processing is currently available [30]. The nature of the impurities depends on the synthesis method, reaction time, type of catalyst, catalyst support and carbon source employed.

One of the applications of CNTs that has received much attention in the literature recently is their use as a catalyst support. When CNTs are used as a catalyst support, the hydrophobic and inert nature of the as-grown CNTs can be unfavourable. It is therefore important to be able to modify their surface chemistry, for example, by the introduction of oxygen-containing surface groups. Upon oxidation, the hydrophobic CNTs become more hydrophilic so that wetting properties are enhanced and the CNT surface becomes more reactive [26,31,32]. Most importantly the dispersion of an active metal phase during catalyst preparation increases with an increasing amount of surface oxygen [26,33]. The presence of carboxyl groups on a CNT surface gives rise to cation-exchange properties [34] which can act as anchor sites for the metal particles. A critical survey of methods most frequently used for the determination of surface-oxygen groups and the use of nitric acid treatment to oxidize carbon surfaces has been given by Boehm [27]. Aqueous solutions of HNO_3 contain nitronium ions, NO_2^+, which are able to attack aromatic compounds and this is assumed to be the first step in the introduction of oxygen-containing surface groups [1]. Although the precise nature of carbon–oxygen structures is not well established, results from many studies demonstrate that several types of surface oxygen-groups can be identified using FTIR spectroscopy, TGA in an inert environment and Boehm mass titration [26,31,32].

The chemical modification of carbon nanotubes represents an emerging research area for nanotube-based materials [35]. In contrast to activated carbons and carbon blacks, the surface oxidation of the relatively new carbon nanotubes and nanofibres has been much less studied [26].

In a study focussed on the use of an Fe/CNT catalyst in Fischer–Tropsch synthesis we observed that this catalyst proved to be easy to use and a stable catalyst with good activity [36]. Scanning transmission electron microscopy (STEM) studies revealed that the surface was heavily pitted and was populated with Fe and, unexpectedly, Ca^{2+} ions [37]. This led us to propose the concept of "docking stations" to explain the remarkable stability of the catalyst [37,38]. These "docking stations" prevent or mitigate sintering which in turn suppresses deactivation. To further explore the origin of the surface roughness of the CNTs produced using $CaCO_3$ as a support, we herein report on a comprehensive investigation of the CNT surface after using a range of acid treatments, unlike previous studies which use relatively severe acid treatments. In particular we have established that a correlation exists between surface roughness induced during acid treatment and the stability and activity of the Fe/CNT catalysts, and that this effect is related to CNT surface roughness.

2. Experimental

2.1. Catalyst preparation

A 10% Fe–Co/$CaCO_3$ catalyst with 5 wt% Fe and 5 wt% Co metal loading was synthesized by the wet impregnation technique [36,38]. In this technique, $Fe(NO_3)_3{\cdot}9H_2O$, $Co(NO_3)_2{\cdot}6H_2O$ and $CaCO_3$ (Sigma–Aldrich) were used to prepare the catalyst. Calculated amounts of the Fe and Co nitrates were mixed and dissolved in distilled water to make a 0.3 M Fe–Co (50:50, w/w) precursor solution. This solution was added dropwise to the $CaCO_3$ support and the mixture was left for 30 min while stirring. The metal–support mixture was then filtered and the product was first left to stand in air for 2 h at room temperature and then dried in a static air oven at 120 °C for 12 h. The product was then removed from the oven and left to cool to room temperature. It was ground and screened through a 150 μm sieve. The catalyst powder obtained was then calcined at 400 °C for 16 h in a static air oven in order to decompose the nitrates.

2.2. Carbon nanotube synthesis

Multiwalled carbon nanotubes were produced by the catalytic decomposition of acetylene (Afrox South Africa) over the 10% Fe–Co/$CaCO_3$ catalyst prepared as described above. Nitrogen (Afrox South Africa) was used as a carrier gas and as a diluent. Previous studies in our research group have focussed on the optimization procedure and effect of various parameters on the synthesis of carbon nanotubes [21]. The optimum conditions were used here for the synthesis of CNTs (see supplementary information for further details).

In the synthesis of multiwalled carbon nanotubes (MWCNTs), approximately 1 g of the catalyst was spread uniformly in a quartz boat (120 mm × 15 mm), which was inserted in the centre of a tubular fixed-bed quartz reactor (length: 510 mm, ID: 19 mm). The reactor, mounted horizontally in an electrical tube furnace, was then heated from room temperature to 700 °C at 10 °C/min while N_2 flowed over the catalyst at 40 ml/min. When the temperature reached 700 °C, the N_2 flowrate was changed to 240 ml/min and acetylene was introduced at a flowrate of 90 ml/min. The reaction was allowed to take place for 60 min, thereafter, the C_2H_2 flow was stopped and the furnace was left to cool down to room temperature under N_2 (40 ml/min). The boat was then removed from the reactor and approximately 3.5 g of black soot was collected.

2.3. Carbon nanotube purification/functionalisation

As-prepared CNTs were refluxed at 120 °C in 30% HNO_3 and 55% HNO_3 for 2 and 6 h respectively (about 2 g of raw material in 200 ml of acid). At the end of the acid treatment, each mixture was diluted with distilled water followed by filtering and washing with distilled water until the pH of the filtrate was ~7. The resulting product was dried in an oven at 120 °C overnight. The four purified materials were named: CNT-30R2 (i.e. CNT refluxed in 30% HNO_3 for 2 h), CNT-30R6, CNT-55R2 and CNT-55R6.

2.4. Characterisation techniques

The morphology and structures of the as-prepared and acid-treated CNTs were characterized by TEM. Sample specimens for TEM studies were prepared by ultrasonic dispersion of the sample in methanol. The suspensions were dropped onto a SPI-carbon coated copper grid. TEM investigations were carried out using a FEI Tecnai Spirit G^2 transmission electron microscope operating at 120 kV. Energy dispersive X-ray (EDX) spectroscopy coupled with TEM was used to confirm the elemental composition of the sample. The inner and outer diameter distributions of the CNTs were

obtained by using Image J software. About 120 CNT diameters were measured per sample.

The zeta potential measurement was used to quantify the electrical potential of the solid particle [39]. Zeta potentials of the as-grown and acid treated CNTs were measured using a Malvern Zetasizer nano-series instrument. CNTs were dispersed in deionised water at room temperature and the pH of the suspension was adjusted from 2.0 to 12.0 by adding 0.1 M hydrochloric acid (HCl) or 0.1 M sodium hydroxide solution (NaOH) solution to the glass beaker containing the CNTs. By measuring the zeta potential as a function of pH, the point of zero charge (the pH value at which the zeta potential is zero, and the CNTs surface is electrically neutral) was determined.

The surface area and pore volume of the as-grown as well as the acid-treated CNTs were determined by N_2 physisorption using a Micromeritics TRISTAR 3000 analyzer. A sample of approximately 300 mg was degassed at 150 °C and 250 °C for 4 h under a flow of N_2, and then the surface area and pore volume were determined by the Brunauer–Emmett–Teller (BET) method as described by Idakiev et al. [40].

The TGA analysis was done on a PerkinElmer STA 4000 analyzer. About 5–10 mg of sample was placed in a ceramic pan and placed in the instrument's furnace. The temperature of the sample was increased from room temperature to 900 °C at 10 °C/min under either an oxidative atmosphere (air, 20 ml/min) or an inert atmosphere (N_2, 20 ml/min). The TGA profile obtained gave information on the sample composition, thermal stability under a specific atmosphere and purity. The derivative curve (DTG) was used to identify the decomposition temperature maxima. The extent to which oxygen was introduced during the purification step was also assessed using thermogravimetric analysis of the CNTs in an inert atmosphere [3].

Raman spectroscopy (Jobin-Yvon T64000 micro-Raman spectrometer) was employed to evaluate the quality of the CNTs.

The presence of oxygen-containing surface groups on the CNTs was established by recording FTIR spectra on a Bruker TENSOR 27 FTIR spectrometer in the 400–4000 cm^{-1} wavenumber range, at a spectral resolution of 4 cm^{-1} using 64 scans per spectrum.

2.5. Fischer–Tropsch experiments

All the catalysts used in the Fischer–Tropsch runs were prepared by the deposition precipitation (DPU) method using urea as the precipitating agent [36,38]. A predetermined amount of $Fe(NO_3)_3{\cdot}9H_2O$ (Sigma–Aldrich) was used to prepare a 10% Fe/CNT sample. The resultant catalysts were dried (120 °C overnight) and calcined (heating in nitrogen at 250 °C for 150 min) to decompose the salts. The catalysts were characterised using BET surface area, H_2 chemisorption, TPR and TEM procedures.

The Fischer–Tropsch synthesis was performed in a fixed-bed micro reactor [41,42]. Gas cylinders containing $H_2/CO/N_2$ mixtures (60% H_2, 30% CO and 10% N_2; purity: 99.99%) were used to supply the reactant gas stream to the catalyst. Nitrogen was used as an internal standard in order to ensure an accurate mass balance.

Catalyst (0.5 g) was added to the reactor and reduced in situ at 350 °C for 20 h under a stream of pure hydrogen (2 bar pressure, 20 ml/min). After reduction the temperature was decreased to 275 °C, the pressure was increased gradually to 8 bar and a flow of syngas was passed over the catalyst bed with a similar flowrate (GHSV = 2400 h^{-1}). All gas lines after the reactor were kept at 150 °C and the hot trap placed immediately after the reactor was held at 150 °C in order to collect wax. A second trap kept at ambient temperature was used to collect the oil and water mixture. The flow of gases was controlled using a metering valve and measured with a bubble meter. The gaseous product stream was analysed online using two gas chromatographs. An offline GC was used to analyse the oil and wax. Data analysis used in our study was performed by standard procedures as described elsewhere [36,42,43].

3. Results and discussion

3.1. Electron microscopy

Among the numerous known techniques employed to synthesise CNTs, CCVD is the most reproducible, cheapest and easily scalable method [16,17]. This method was therefore used in this study to synthesise CNTs. The majority of the tubes had outer diameters ranging from 20 to 35 nm and inner diameters ranging from 8 to 18 nm (Figs. 1 and 2). After acid treatment using the harshest oxidizing condition (sample CNT-55R6), the CNT inner diameter hardly changed but the outer diameter decreased relative to the non acid treated sample. This reduction in diameter is due to the interaction of acid with the outermost graphene layers (Fig. 2). The decreased outer diameter is also attributed to wall damage during acid treatment and this is confirmed by TEM micrographs (Fig. 3).

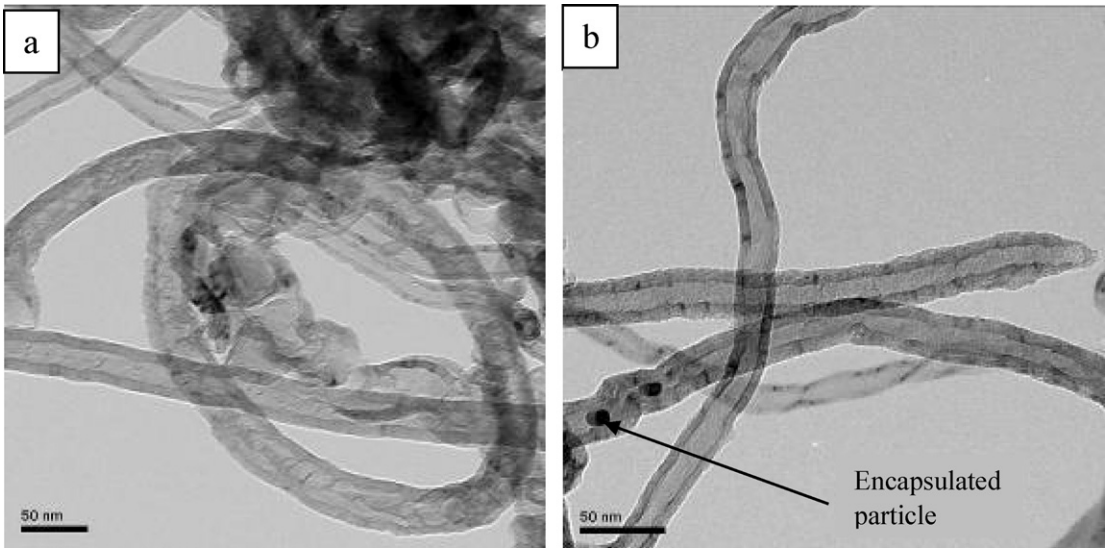

Fig. 1. TEM images of (a) as-grown CNTs and (b) as-grown CNTs showing some encapsulated metal particles indicated by arrow.

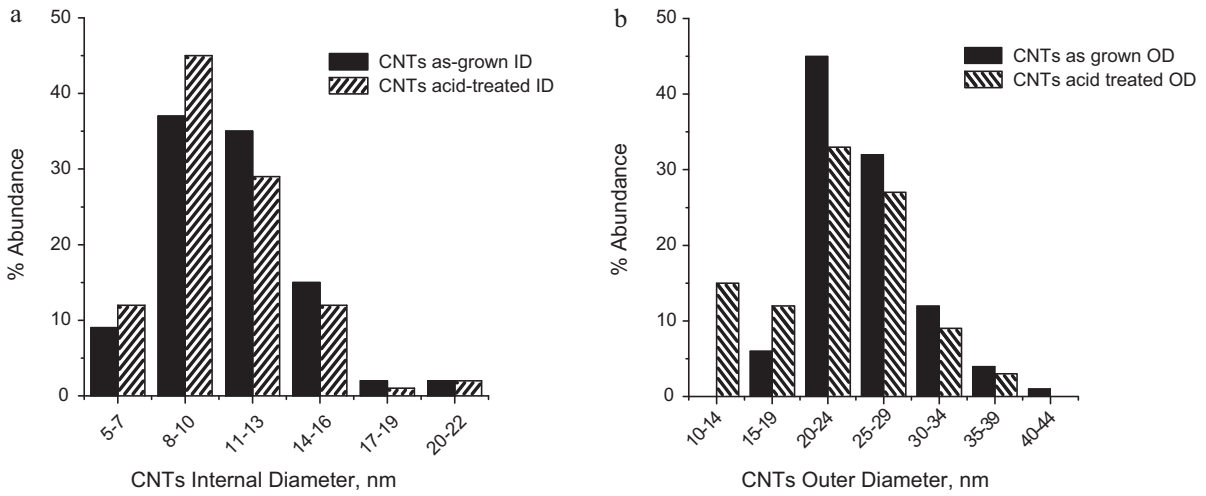

Fig. 2. Diameter size distribution before and after acid treatments. (a) Comparison of inner diameters and (b) comparison of outer diameters.

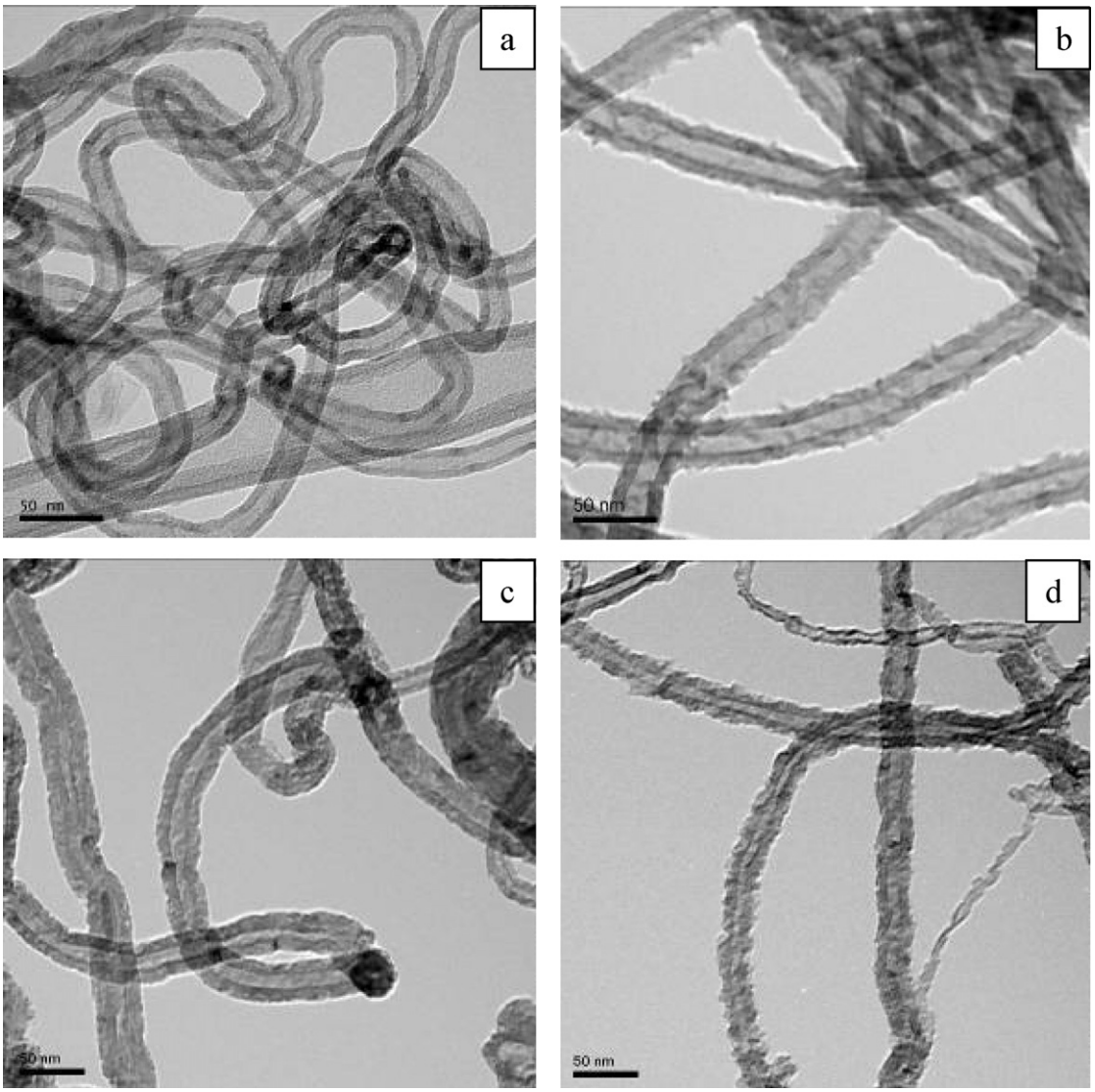

Fig. 3. Effect of acid treatment on the texture and morphologies of CCVD synthesised CNTs: (a) CNTs-30R2, (b) CNT-30R6, (c) CNT-55R2, and (d) CNT-55R6.

Table 1
Point of zero charge (PZC) obtained from zeta potential measurements.

Sample	PZC
As grown CNTs[a]	4.9
CNT-30R2	2.9
CNT-30R6	2.7
CNT-55R2	2.5
CNT-55R6	<0

[a] PZC = 5.0 [39].

TEM images of the as-grown CNTs (Fig. 1b and Figure S2) reveal encapsulated metal particles which were shown by EDX analysis to be Fe and Co (Figure S1a-supporting information). After acid treatment, the residual catalyst was removed (Figure S1b-supporting information) due to the dissolution of the metal catalysts by nitric acid. However removal of all the Fe and Co catalyst that was observed within the tubes was not possible. The TEM images also revealed that the roughness increased with nitric acid concentration and time of reaction. The tubes became thinner and the surface rougher (Fig. 3a–d and Figure S3).

3.2. Zeta potential measurements

The determination of the zeta potential of the CNTs can be used to study the presence of oxygen surface groups. The presence of acidic groups causes the carbon surface to be more hydrophilic, increasing the negative surface charge density and decreasing the pH of the point of zero charge (PZC) [34,44]. Fig. 4 shows the plots of zeta potential of the as-grown and oxidised CNTs as a function of pH. The PZC for the as-grown CNT occurs at pH 4.9. That is at pH < 4.9, the surface of the CNTs is positively charged and at pH > 4.9, the surface is negatively charged. This result is in good agreement with results obtained by Li et al. [39] (see footnote to Table 1). After acid treatment, the PZC shifts to lower pH values due to the introduction of surface oxygen groups (Table 1). CNT-30R2, CNT-30R6 and CNT-55R2 all have values very close to a pH_{pzc} around 2.6 with CNT-55R6 having the lowest PZC. These results suggest that acidic functional groups are formed on the carbon nanotubes surface and their concentration increases with treatment time and acid strength.

3.3. Surface area and pore volume measurements

Nitrogen adsorption represents the most widely used technique to determine a materials' surface area and to characterize its porous structure [45]. The surface area and pore volume of the as-grown and acid-treated CNTs are given in Table 2. Prior to the surface area and pore volume analysis, the effect of degassing temperature was investigated and it was demonstrated that whether the sample is degassed at 150 °C or at 250 °C for 4 h the surface area and pore volume values are the same within experimental error (Table 2). The surface area and pore volume increased with the initial acid treatment due to the removal of the low surface area residual CaO and possibly opening of the ends of the tubes, but did not change significantly on further treatment.

3.4. Thermogravimetric analysis (TGA)

Thermogravimetric analysis (TGA), coupled with a derivative curve of the weight loss (DTG), is often used to investigate the thermal stability as well as the composition and purity of carbons. It is an effective way to quantitatively evaluate CNTs, in particular, the content of residual metal. It is easy to obtain the residual metal content using this technique by simply oxidising the CNT samples in air. The carbon material is converted to CO/CO_2 and the metal catalyst is converted to an oxide [46].

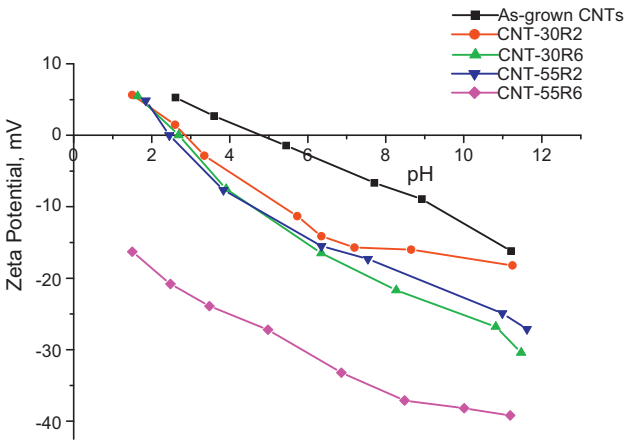

Fig. 4. Zeta potential measurements of as-grown and acid treated CNTs as a function of pH.

Fig. 5 shows the TGA and DTG profiles of the as-grown CNTs. The residual catalyst and CaO makes up ~17% of the mass so that 83% of the sample is due to carbonaceous materials. There is no significant weight loss before 500 °C in the as-grown CNTs, thus ruling out the presence of a significant amount of amorphous carbon. In the product, the greatest rate of carbon decomposition occurs at 642 °C with a small peak in the derivative curve at 729 °C as seen from Fig. 5. This is a typical decomposition profile for multiwalled carbon nanotubes (MWCNTs) [46], and confirms that the carbon nanotubes were multiwalled. The small proportion of CNTs oxidising at the higher temperature could be those CNTs not in proximity to residual catalyst or due to the presence of some highly graphitised carbon.

After refluxing in nitric acid, the impurity content decreased to less that 1%, with values dependent on the treatment time and acid strength. Figs. 6 and 7 show an increase in sample mass at 500 °C due to the oxidation of residual Fe–Co metal; the derivative peak breadth showed an increase upon oxidation due to an increase in the number of defects. When the as-grown CNTs were refluxed in 30% HNO_3 for 2 h and 6 h, the thermal stability of the CNTs improved slightly (Fig. 6) and the temperature at which the rate of CNT decomposition is a maximum increased from 642 °C to 685 °C and 690 °C, respectively. This increase in thermal stability is attributed to the removal of catalyst which is known to aid the oxidation of carbon. On the other hand, when the as-grown CNTs were refluxed in 55% HNO_3 for 2 and 6 h, the thermal stability maxima of the CNTs decreased slightly with the decomposition temperature

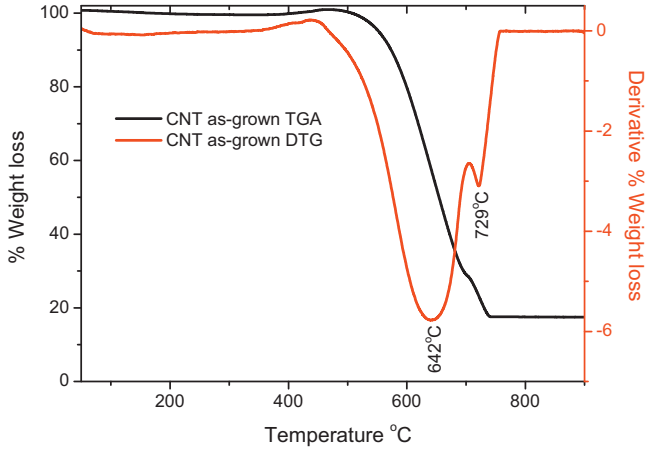

Fig. 5. TGA and DTG profiles of as-grown CNTs under air atmosphere.

Table 2
Surface area and pore volume of as-grown and acid-treated CNTs.

Sample ID	Degassed under N_2 at 150 °C[a]		Degassed under N_2 at 250 °C[a]	
	BET surface area (m^2/g)[b]	Pore volume (cm^3/g)	BET surface area (m^2/g)[b]	Pore volume (cm^3/g)
CNT-as grown	80	0.27	77	0.27
CNT-30R2	105	0.34	103	0.35
CNT-30R6	112	0.35	114	0.34
CNT-55R2	108	0.35	–	–
CNT-55R6	100	0.33	–	–

[a] 4 h.
[b] ±5% experimental error.

Table 3
Weight loss of CNTs due to the formation of CO/CO_2 on heating in N_2.

Sample ID	150–400 °C %CO_2	100–900 °C %(CO_2 + CO)
CNT as-grown	0.95	8.36
CNT-30R2	1.81	11.04
CNT-30R6	2.75	15.14
CNT-55R2	3.52	19.95
CNT-55R6	4.27	18.78

dropping to 633 and 639 °C for the 2 h and 6 h treatments, respectively (Fig. 7), although the purity of the CNTs was improved. The drop in temperature can be attributed to the damage of the outer structure as confirmed by TEM and Raman spectroscopy. These observations suggest that acid concentration and not temperature has the more significant effect on achieving wall defects on CNTs. In summary, the position of the decomposition peak maximum is affected by the amount of residual catalyst in the sample, the defect content on the surface of the CNTs and the amount of amorphous carbon present.

TGA profiles of the as-grown as well as the acid-treated CNTs were also recorded under a N_2 atmosphere in order to determine the oxygen surface group content on the CNTs. The weight loss occurring from 150 °C to 400 °C corresponds to the evolution of gaseous CO_2 [47] while the total weight loss from 100 °C to 900 °C was correlated with the weight loss due to the formation of both CO and CO_2 [3] (Fig. 8). The derivative curve for the acid treated samples is shown in Fig. 8b. The weight loss below 100 °C is due to H_2O loss, between 150 and 400 °C CO_2 is evolved from acid (COOH) groups and the weight loss at temperature >400 °C could be due to the loss of oxygen atoms tightly bonded to the surface of the CNTs or other non-graphitic carbonaceous species.

Table 3 shows the % CO_2 and CO formed during the experiment which corresponds to the weight loss of CNTs in a N_2 atmosphere. The weight loss is plotted against the reflux time in Fig. 9, showing an increase in the amount of CO_2 evolved with increasing reflux time and acid concentration. A similar trend was observed by de Jong and Geus when working with carbon nanofibers [3].

3.5. Raman spectroscopy

Raman spectral analysis was used to determine the long range structure of the CNTs [48,49]. A major drawback of Raman spectroscopy is that it cannot provide direct information on the nature of metal impurities, and it is not very effective in studying CNT samples with a low content of amorphous carbon [50,51]. However, Raman spectra for as-grown as well as acid-treated CNTs show two characteristic peaks in all samples, one at ~1350 cm^{-1} corresponding to the disorder-induced band (D band) and the other at ~1590 cm^{-1} corresponding to the tangential mode (G band) (Fig. 10). The D mode indicates the disorder features of the CNTs whereas the G mode is associated with the ordered graphite in the CNTs [52]. The area ratio of the D band to the G band (I_D/I_G) was used to estimate the amount of disorder or defects present in the walls of the CNTs. The (I_D/I_G) ratio was found to increase with increasing reflux time/acid strength indicating that the longer the reflux time, the more defects are added to the CNTs. These results are in good agreement with the TEM observations.

Table 4
Raman data for as-grown and acid-treated CNTs.

Sample ID	Peak position (cm^{-1})		I_D/I_G
	D-band	G-band	
CNT as-grown	1345	1599	2.88
CNT-30R6	1354	1598	2.83
CNT-55R2	1353	1583	2.41
CNT-55R6	1354	1583	3.79

Error bar ± 2 cm^{-1}.

Table 4 shows the position of the D and G band as well as the ratio of areas for the as-grown and acid treated CNTs. From the results, it is observed that there is an upfield shift of the D-band for the acid-treated CNTs with respect to the as-grown CNTs. Similar observations were obtained by Okpalugo et al. and correlated with the inter-tubular coupling resulting from Van der Waals repulsions [53].

3.6. FTIR analysis

FTIR spectroscopy is a very useful and direct technique for the study of the nature of oxygen surface groups. However there are well-known experimental difficulties involved in obtaining IR spectra of carbon materials [33]. FTIR can only be used for highly oxidised carbon surfaces; otherwise the intensity of the absorption bands is very poor [54]. The FTIR data are presented in Fig. 11. When comparing the FTIR spectra, peaks appear at 1737 cm^{-1}, 1364 cm^{-1} and 1217 cm^{-1} for the acid-treated CNTs relative to the as-grown CNTs. This clearly shows that acid treatment has introduced some functional groups onto the surface of the CNTs. The amount of these functional groups present on the surface depends on the reflux time and/or the acid strength. The peak appearing at ~1737 cm^{-1} can be ascribed to the C=O stretching vibration of carboxyl or carbonyl groups [55–57] while that at 1364 cm^{-1} is associated with NO_2 stretching vibrations [58,59] and the peak at 1217 cm^{-1} corresponds to C–O stretching and O–H bending vibrations [55–57]. It can be concluded that FTIR analysis also provides evidence for the existence of defects in the walls of the CNTs. This result is in good agreement with the Raman analysis.

3.7. Fischer–Tropsch data

A series of 10% Fe/CNT catalysts was made using a deposition precipitation procedure with urea. The five catalysts (Fe/CNT-55R6, Fe/CNT-55R2, Fe/CNT-30R6, Fe/CNT-30R2, and Fe/CNT-as grown) were calcined and reduced using standard procedures (see Section 2). All FT reactions were performed under a set of standard conditions (275 °C, 8 bar, H_2:CO = 2, and GHSV = 2400 h^{-1}). Fig. 12 shows a plot of the catalytic activity in terms of the percentage conversion of CO, as a function of time on stream. (See Figures S4 and S5 and Tables S1 and S2 for characterisation data for these catalysts.) The conversion for all the catalysts was initially low and increased significantly before levelling off within 10 h on stream; afterward the catalyst remained relatively stable for the entire experiment (15–120 h). A comparison of the FTS data obtained from the 10% catalysts prepared on differently functionalised CNTs (Table 5) reveals that the %CO conversions, FT activity and hydrocarbons selectivity are all dependent on the support acid pre-treatment. Thus, the 10% Fe/CNT-as grown catalyst not only has the poorest FT performance but the highest methane selectiv-

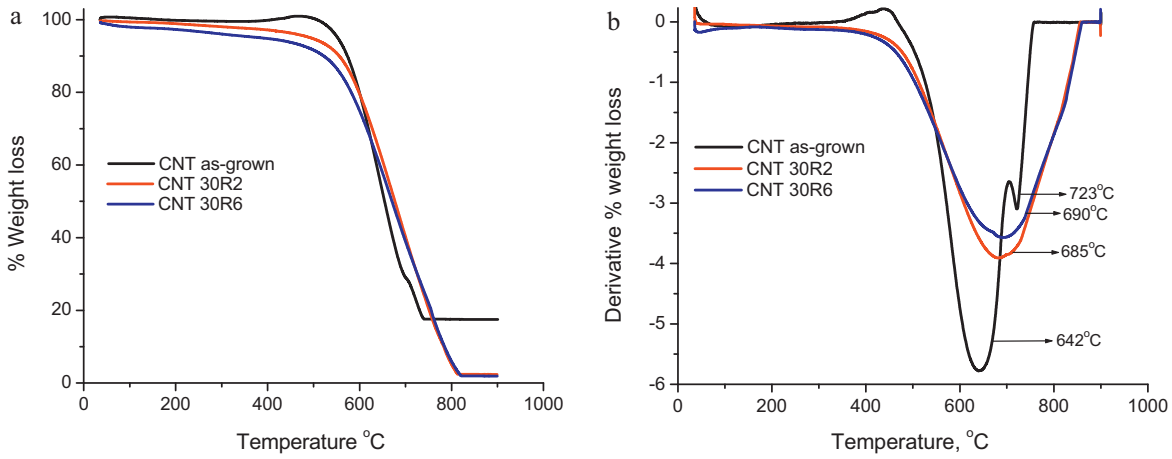

Fig. 6. (a) TGA and (b) DTG profiles of as-grown CNTs as well as purified CNTs in 30% HNO_3 under air atmosphere.

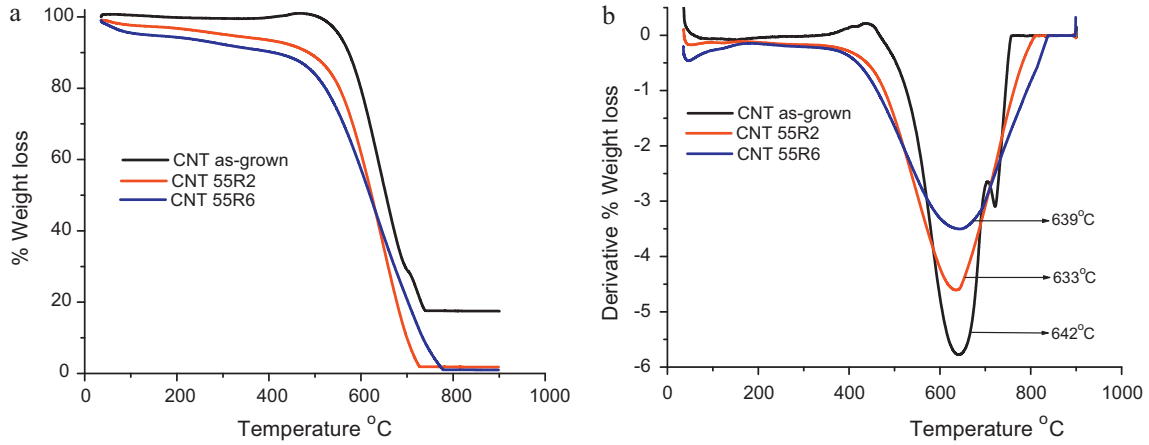

Fig. 7. (a) TGA and (b) DTG profiles of as-grown CNTs as well as purified CNTs in 55% HNO_3 under air atmosphere.

ity and lowest C_{5+} product selectivity of the tested catalysts. The FT activity data presented in Table 5 is given per g of catalyst, rather than as a turnover frequency. Attempts to use H_2 chemisorption to determine the surface area of the active metal were unsuccessful, presumably because the particles are too small [37], as reflected by TEM. Consequently the turnover frequency could not be calculated.

It was observed that the FT activity increased with increasing amount of oxygen functional groups on the support, i.e. the FT activity followed the order Fe/CNT-55R6 > Fe/CNT-55R2 > Fe/CNT-30R6 > Fe/CNT-30R2 > Fe/CNT-as grown. From the zeta potential measurements, it can be seen that CNT-55R6 has the highest concentration of negative charge and should lead to the best Fe dispersion; this is also the catalyst with the highest activity. The better

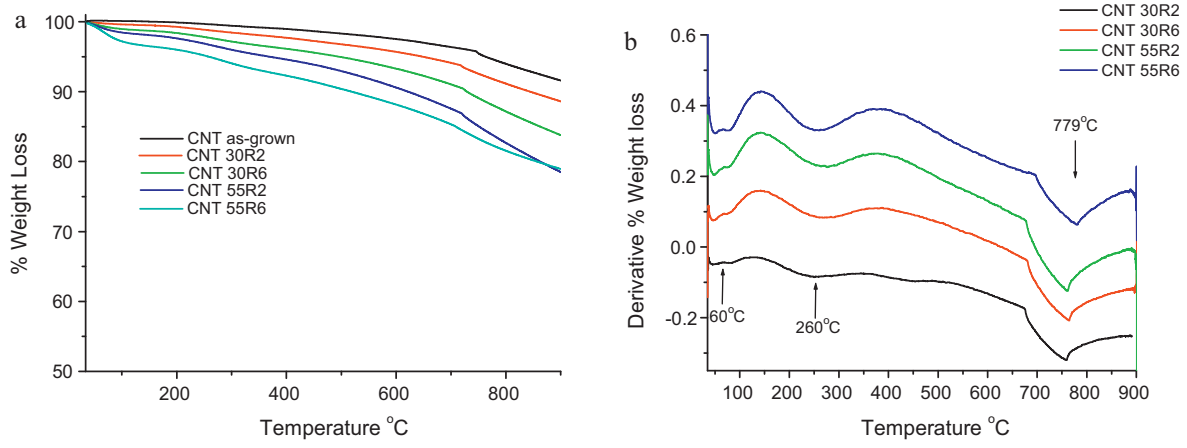

Fig. 8. (a) TGA and (b) DTG profiles of as-grown and acid treated CNTs under N_2 atmosphere.

Table 5
Activity and selectivity of iron catalyst supported on differently functionalized CNTs in Fischer–Tropsch synthesis.

Catalyst	%CO conversion	FT activity (μmol/min gCat)	Hydrocarbons selectivity (mol%)				
			C_1	C_2	C_3	C_4	C_{5+}
10% Fe/CNT-as grown	20	71	48	15	13	7.7	17
10% Fe/CNT-30R2	29	153	30	15	19	13	24
10% Fe/CNT-30R6	35	179	31	8.0	7.3	3.6	50
10% Fe/CNT-55R2	44	214	29	8.4	6.0	2.6	54
10% Fe/CNT-55R6	59	322	19	8.3	9.2	5.4	58

Conditions: 8 bar, 275 °C, CO:H_2 = 1:2, and GHSV = 2400 h^{-1}.

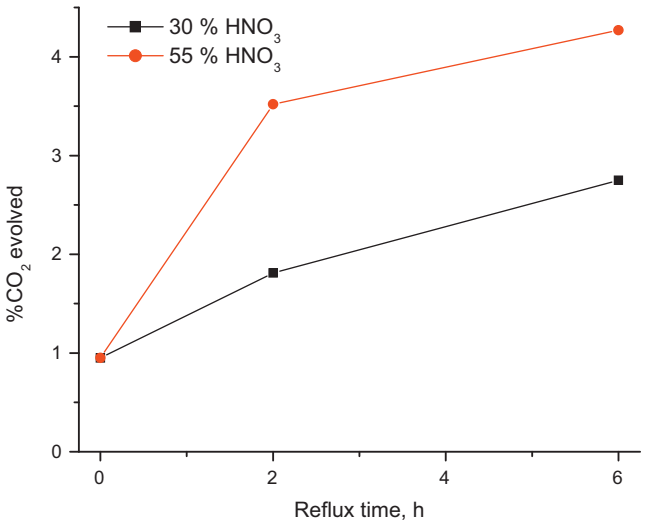

Fig. 9. Evolution of oxygen containing CO_2 versus reflux time.

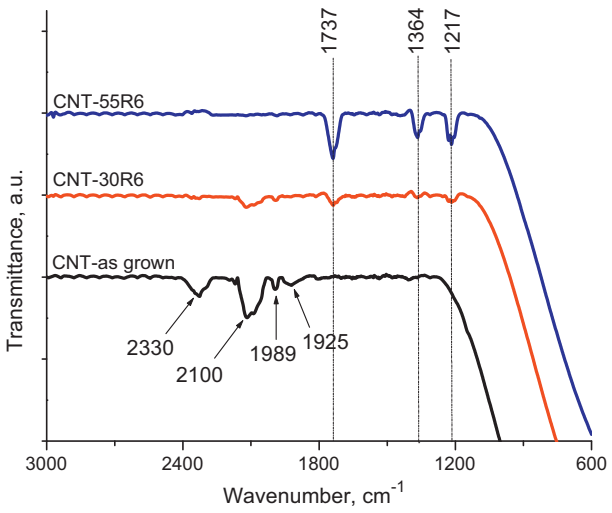

Fig. 11. FTIR spectra of untreated (CNT-as grown) and oxidised carbon nanotubes.

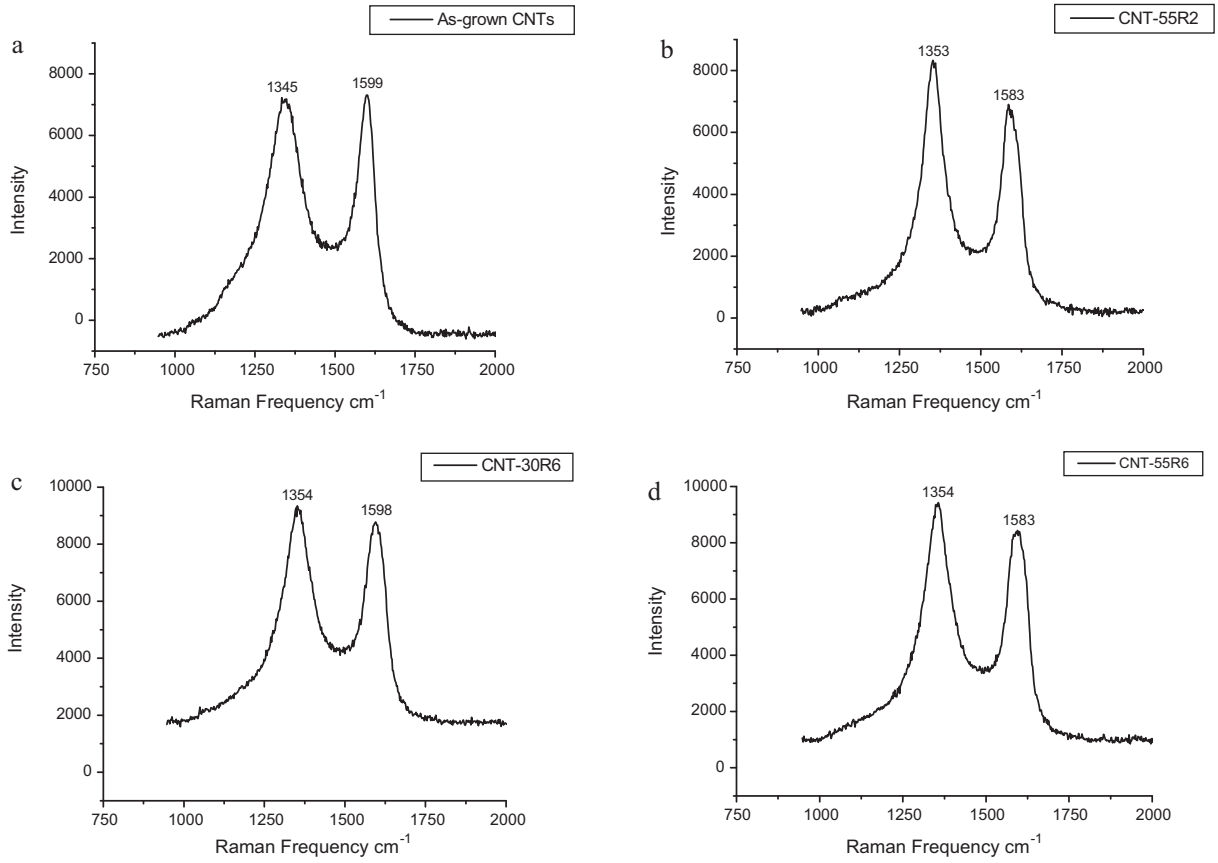

Fig. 10. Raman spectra of CNTs: (a) as-grown CNTs, (b) CNT-55R2, (c) CNT-30R6, and (d) CNT-55R6.

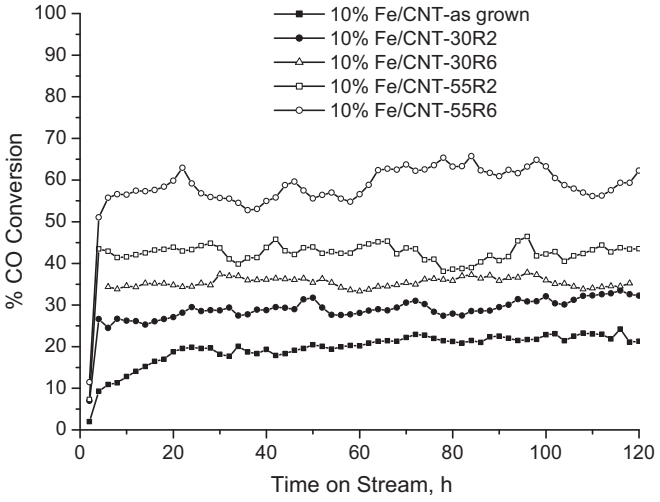

Fig. 12. CO conversion with time on stream.

dispersion of the metal particles on the surface of CNT-55R6 is due to the availability of the extra anchoring sites for the Fe particles, leading to the smaller Fe particles [37] and the better performance during FTS.

This study thus reveals that CNTs that are functionalised using vigorous acid treatments generate *stable* carbon materials that can be used as supports in catalytic reactions. The role of the acid treatment is to create roughened carbon surfaces that facilitate metal binding to the surface through COOH (and possibly OH) groups. The study thus confirms the earlier proposals relating to the role of 'docking stations' generated by acid treatment of CNTs [37].

4. Conclusions

Carbon nanotubes were successfully synthesized using the CCVD method. The as-grown CNTs were purified by refluxing the obtained product in nitric acid. Purification not only removes the impurities, but also introduces oxygenated surface groups onto the CNTs. The presence of those groups altered the surface chemistry of CNTs. The different oxygen functional groups on the CNT surfaces were qualitatively identified by FTIR spectroscopy. Their presence was also detected by Raman spectroscopy where the amount of disorder was related to the presence of surface defects introduced by nitric acid treatment. Zeta potential measurements show that the PZC decreased with treatment time/acid strength indicating an increase in surface acid groups with time. Thermogravimetric analysis revealed that the CNTs produced were multiwalled as indicated by the oxidation temperature profiles typical of MWCNTs. The amount of CO_2/CO desorbed from the surface of CNTs was a function of CNTs treatment time/acid strength. Refluxing CNTs in HNO_3 is suitable for the creation of surface functional groups. In summary, acid treatment of CNTs produced from Fe–Co on $CaCO_3$ can readily generate roughened CNT surfaces and these carbons can be used as stable supports for Fischer–Tropsch catalysts as shown here and in other studies [37]. The activity of the FT catalysts correlates with the degree of acid functionalisation of the support, indicating that the surface groups introduced during the acid treatment are linked to the active sites.

Acknowledgements

The authors wish to thank the Andrew W. Mellon Foundation, the National Research Foundation of South Africa and the University of the Witwatersrand for research funds.

Appendix A. Supplementary data

Supplementary data associated with this article can be found, in the online version, at doi:10.1016/j.molcata.2010.11.033.

References

[1] M.L. Toebes, J.M.P. van Heeswijk, J.H. Bitter, A. Jos van Dillen, K.P. de Jong, Carbon 42 (2004) 307.
[2] J.H. Zhou, Z.J. Sui, J. Zhu, P. Li, D. Chen, Y.C. Dai, W.K. Yuan, Carbon 45 (2007) 785.
[3] K.P. De Jong, J.W. Geus, Catal. Rev. Sci. Eng. 42 (2000) 481.
[4] M.L. Toebes, J.H. Bitter, A.J. van Dillen, K.P. de Jong, Catal. Today 76 (2002) 33.
[5] S. Iijima, Nature 354 (1991) 56.
[6] H. Dai, Acc. Chem. Res. 35 (2002) 1035.
[7] M.S. Dresselhaus, G. Dresselhaus, P.C. Eklund, D.E.H. Jones, Science of Fullerenes and Carbon Nanotubes, Academic Press, San Diego, 1996, pp. 1–985.
[8] A. Thess, R. Lee, P. Nikolaev, H. Dai, P. Petit, J. Robert, C.H. Xu, Y.H. Lee, S.G. Kim, A.G. Rinzler, D.T. Colbert, G.E. Scuseria, D. Tomanek, J.E. Fischer, R.E. Smalley, Science 273 (1996) 483.
[9] T.W. Ebbesen, P.M. Ajayan, Nature 358 (1992) 220.
[10] C. Journet, W.K. Maser, P. Bernier, A. Loiseau, M.L. delaChapelle, S. Lefrant, P. Deniard, R. Lee, J.E. Fischer, Nature 388 (1997) 756.
[11] C. Bower, O. Zhou, W. Zhu, D.J. Werder, S. Jin, Appl. Phys. Lett. 77 (2000) 2767.
[12] S.S. Fan, M.G. Chapline, N.R. Franklin, T.W. Tombler, A.M. Cassell, H.J. Dai, Science 283 (1999) 512.
[13] M. Su, B. Zheng, J. Liu, Chem. Phys. Lett. 322 (2000) 321.
[14] Z.F. Ren, Z.P. Huang, J.W. Xu, J.H. Wang, P. Bush, M.P. Siegal, P.N. Provencio, Science 282 (1998) 1105.
[15] Z. Li, E. Dervishi, Y. Xu, X. Ma, V. Saini, A.S. Biris, R. Little, A.R. Biris, D. Lupu, J. Chem. Phys. 129 (2008) 074712.
[16] A. Magrez, J.W. Seo, C. Miko, K. Hernadi, L. Forro, J. Phys. Chem. B 109 (2005) 10087.
[17] E. Couteau, K. Hernadi, J.W. Seo, L. Thiên-Nga, C. Mikó, R. Gaál, L. Forró, Chem. Phys. Lett. 378 (9) (2003).
[18] S. Porro, S. Musso, M. Giorcelli, A. Chiodoni, A. Tagliaferro, Phys. E: Low-dimen. Syst. Nanostruct. 37 (2007) 16.
[19] H. Kathyayini, N. Nagaraju, A. Fonseca, J.B. Nagy, J. Mol. Catal. A: Chem. 223 (2004) 129.
[20] J.A. Seo, E. Couteau, P. Umek, K. Hernadi, P. Marcoux, B. Lukic, L. Forro, New J. Phys. 5 (2003) 120.
[21] S.D. Mhlanga, K.C. Mondal, R. Carter, M.J. Witcomb, N.J. Coville, S. Afr. J. Chem. 62 (2009) 67.
[22] M. Kumar, Y. Ando, J. Nanosci. Nanotechnol. 10 (2010) 3739.
[23] S.D. Mhlanga, N.J. Coville, Diamond Relat. Mater. 17 (2008) 1489.
[24] D. Vairavapandian, P. Vichchulada, M.D. Lay, Anal. Chim. Acta 626 (2008) 119.
[25] I.D. Rosca, F. Watari, M. Uo, T. Akasaka, Carbon 43 (2005) 3124.
[26] T.G. Ros, A.J. Van Dillen, J.W. Geus, D.C. Koningsberger, Chem. Eur. J. 8 (2002) 1151.
[27] H.P. Boehm, Carbon 40 (2002) 145.
[28] K. Esumi, M. Ishigami, A. Nakajima, K. Sawada, H. Honda, Carbon 34 (1996) 279.
[29] P. Serp, M. Corrias, P. Kalck, Appl. Catal. A: Gen. 253 (2003) 337.
[30] W. Chen, J. Li, L. Liu, Z. Jia, Y. Yu, Z. Zhang, J. Appl. Electrochem. 33 (2003) 755.
[31] H.P. Boehm, Adv. Catal. Relat. Subjects 16 (1966) 179.
[32] F. Rodríguez-Reinoso, Carbon 36 (1998) 159.
[33] C. Prado-Burguete, A. Linares-Solano, F. Rodriguez-Reinoso, C. de Lecea, J. Catal. 115 (1989) 98.
[34] H.P. Boehm, Carbon 32 (1994) 759.
[35] Y.P. Sun, K. Fu, Y. Lin, W. Huang, Acc. Chem. Res. 35 (2002) 1096.
[36] M.C. Bahome, L.L. Jewell, D. Hildebrandt, D. Glasser, N.J. Coville, Appl. Catal. A: Gen. 287 (2005) 60.
[37] U.M. Graham, A. Dozier, R.A. Khatri, M.C. Bahome, L.L. Jewell, S.D. Mhlanga, N.J. Coville, B.H. Davis, Catal. Lett. 129 (2009) 39.
[38] E. van Steen, F.F. Prinsloo, Catal. Today 71 (2002) 327.
[39] Y.H. Li, S. Wang, Z. Luan, J. Ding, C. Xu, D. Wu, Carbon 41 (2003) 1057.
[40] V. Idakiev, Z.Y. Yuan, T. Tabakova, B.L. Su, Appl. Catal. A: Gen. 281 (2005) 149.
[41] M.E. Dry, Appl. Catal. A: Gen. 138 (1996) 319.
[42] D.J. Duvenhage, N.J. Coville, Appl. Catal. A: Gen. 153 (1997) 43.
[43] R.M.M. Abbaslou, A. Tavasoli, A.K. Dalai, Appl. Catal. A: Gen. 355 (2009) 33.
[44] C. Moreno-Castilla, M.A. Ferro-Garcia, J.P. Joly, I. Bautista-Toledo, F. Carrasco-Marin, J. Rivera-Utrilla, Langmuir 11 (1995) 4386.
[45] G. Leofanti, M. Padovan, G. Tozzola, B. Venturelli, Catal. Today 41 (1998) 207.
[46] A.R. Harutyunyan, B.K. Pradhan, J. Chang, G. Chen, P.C. Eklund, J. Phys. Chem. B 106 (2002) 8671.
[47] M.N. Kirikova, A.S. Ivanov, S.V. Savilov, V.V. Lunin, Russ. Chem. Bull. 57 (2008) 298.
[48] J. Kastner, T. Pichler, H. Kuzmany, S. Curran, W. Blau, D.N. Weldon, M. Delamesiere, S. Draper, H. Zandbergen, Chem. Phys. Lett. 221 (1994) 53.
[49] F.X. Wang, X.P. Gao, Z.W. Lu, S.H. Ye, J.Q. Qu, F. Wu, H.T. Yuan, D.Y. Song, J. Alloys Compd. 370 (2004) 326.
[50] P.X. Hou, C. Liu, H.M. Cheng, Carbon 46 (2008) 2003.
[51] T.J. Park, S. Banerjee, T. Hemraj-Benny, S.S. Wong, J. Mater. Chem. 16 (2006) 141.

[52] A. Jorio, M.A. Pimenta, A.G. Souza Filho, R. Saito, G. Dresselhaus, M.S. Dresselhaus, New J. Phys. 5 (2003) 139.
[53] T.I.T. Okpalugo, P. Papakonstantinou, H. Murphy, J. Mclaughlin, N.M.D. Brown, Carbon 43 (2005) 2951.
[54] S. Kundu, Y. Wang, W. Xia, M. Muhler, J. Phys. Chem. C 112 (2008) 16869.
[55] W.M. Prest, R.A. Mosher, Anonymous Colloids and Surfaces in Reprographic Technology ACS Symposium Series, 1982.
[56] P. Painter, M. Starsinic, M. Coleman, IV, In: J.R. Ferraro, L.L. Basile (Eds.), Fourier Transform Infrared Spectra Vol. 4: Applications to Chemical Systems (Fourier Transform Infrared Spectroscopy) Academic Press, Orlando, 1985, p. 169.
[57] M.S.P. Shaffer, X. Fan, A.H. Windle, Carbon 36 (1998) 1603.
[58] U. Zielke, K.J. Hüttinger, W.P. Hoffman, Carbon 34 (1996) 983.
[59] M.M. Keyser, F.F. Prinsloo, in: B.H. Davis, M.L. Occelli (Eds.), Studies on Surface Science Catalysis, Elsevier, 2007, p. 45.